Article

Electrochemical and Ion Transport Studies of Li⁺ Ion-Conducting MC-Based Biopolymer Blend Electrolytes

Elham M. A. Dannoun [1], Shujahadeen B. Aziz [2,3,*], Mohamad A. Brza [4], Sameerah I. Al-Saeedi [5], Muaffaq M. Nofal [6], Kuldeep Mishra [7], Ranjdar M. Abdullah [2], Wrya O. Karim [8] and Jihad M. Hadi [9]

[1] Associate Chair of the Department of Mathematics and Science, Woman Campus, Prince Sultan University, P.O. Box 66833, Riyadh 11586, Saudi Arabia
[2] Hameed Majid Advanced Polymeric Materials Research Lab., Physics Department, College of Science, University of Sulaimani, Qlyasan Street, Kurdistan Regional Government, Sulaimani 46001, Iraq
[3] The Development Center for Research and Training (DCRT), University of Human Development, Sulaimani 46001, Iraq
[4] Medical Physics Department, College of Medicals & Applied Science, Charmo University, Chamchamal, Sulaimani 46023, Iraq
[5] Department of Chemistry, College of Science, Princess Nourah bint Abdulrahman University, P.O. Box 84428, Riyadh 11671, Saudi Arabia
[6] Department of Mathematics and Science, Prince Sultan University, P.O. Box 66833, Riyadh 11586, Saudi Arabia
[7] Department of Physics, Jaypee University, Anupshahar 203390, Uttar Pradesh, India
[8] Department of Chemistry, College of Science, University of Sulaimani, Qlyasan Street, Kurdistan Regional Government, Sulaimani 46001, Iraq
[9] Nursing Department, College of Nursing, University of Human Development, Kurdistan Regional Government, Sulaimani 46001, Iraq
* Correspondence: shujahadeenaziz@gmail.com

check for updates

Abstract: A facile methodology system for synthesizing solid polymer electrolytes (SPEs) based on methylcellulose, dextran, lithium perchlorate (as ionic sources), and glycerol (such as a plasticizer) (MC:Dex:LiClO₄:Glycerol) has been implemented. Fourier transform infrared spectroscopy (FTIR) and two imperative electrochemical techniques, including linear sweep voltammetry (LSV) and electrical impedance spectroscopy (EIS), were performed on the films to analyze their structural and electrical properties. The FTIR spectra verify the interactions between the electrolyte components. Following this, a further calculation was performed to determine free ions (FI) and contact ion pairs (CIP) from the deconvolution of the peak associated with the anion. It is verified that the electrolyte containing the highest amount of glycerol plasticizer (MDLG3) has shown a maximum conductivity of 1.45×10^{-3} S cm^{-1}. Moreover, for other transport parameters, the mobility (μ), number density (n), and diffusion coefficient (D) of ions were enhanced effectively. The transference number measurement (TNM) of electrons (t_{el}) was 0.024 and 0.976 corresponding to ions (t_{ion}). One of the prepared samples (MDLG3) had 3.0 V as the voltage stability of the electrolyte.

Keywords: biopolymer blend electrolyte; EIS and FTIR; ion transport parameters; complex permittivity; LSV and TNM measurements

1. Introduction

Due to demand for high-energy consumption, for instance, to power laptops and mobile devices, the usage of energy storage devices is widespread. In order to produce low-cost and safe energy storage systems, the design of high-performance electrochemical devices has been extensively studied [1,2]. It is essential to use polymer electrolytes (PEs) for electrochemical devices because of their common advantages including qualities such as wide electrochemical windows, leakage-free, ability to form thin films, lightweight, flexibility, ease of handling, transparency, good conductivity, and solvent-free feature compared to commercial liquid electrolytes (LEs) [3,4]. In the PEs of the energy storage

devices, the host polymer is often divided into two types: natural and synthetic polymers [5]. Non-biodegradable synthetic polymers deplete petroleum resources and introduce disposal difficulties [6]. As a result, biopolymers may be employed as the host polymer to investigate energy storage devices and minimize plastic waste pollution. These polymers, which derive from natural resources, have distinct advantages over synthetic ones, including low cost, wide compatibility with a wide range of solvents, abundance, and high film formation efficiency [7,8]. In PE investigations, starch, cellulose, chitosan, dextran, and carrageenan are the most- often employed biopolymers [9–13].

The search for novel ion-conducting PEs for lithium-based energy devices continues incessantly [14–17]. To replace the LEs in lithium-ion batteries, PEs that are linked to lithium salts and integrated into neutral or ion-conducting polymers have been suggested [18]. In contrast to manufactured polymers, which are durable, natural biopolymers degrade with time [19]. Cellulose is nature's most abundant organic polymer, making it an excellent source of renewable energy [8]. As a natural polymer, cellulose is seen as a potential replacement for petrochemical polymers [20]. Cyanoacrylate is one of the most often used and lowest-priced types of cellulose. A biodegradable polymer that has excellent film-forming capabilities may be transparent and possesses superior mechanical and electrical properties that can be made from alkali cellulose. Methylcellulose (MC) is one of these cellulose derivatives [6]. By adding dimethyl sulfate or methyl chloride to alkali-based cellulose, a polymer with a 1,4 glycosidic link is created, known as MC [21]. Through a dative connection, ions create a complexation with polymer-host-oxygen-containing functional groups. Ion conduction in MC is facilitated by functional groups possessing lone-pair electrons, including hydroxyl, glycosidic link, and mexthoxy groups [22]. When it comes to film-forming and dissolving qualities, MC is a standout because of its strong mechanical, thermal, and chemical stabilities [23]. Glass transition temperature (Tg) for microcrystalline MC is between 184 and 200 °C, making it an excellent material for high-temperature applications [22]. Leuconostoc mesenteroides bacteria produce dextran, a non-toxic and biodegradable polysaccharide that has lone-pair electrons of heteroatoms, such as oxygen, which is essential for dissolving inorganic salts [13]. The polymer blend approach has been reported to generate a polymer mix host with higher ionic conduction sites [24]. A reduced glass transition temperature and degree of crystallinity may be achieved by mixing polymers [25]. A PE based on lithium salts is able to perform well overall in terms of crucial features, such as electrochemical window stability and ionic conductivity [26]. Various plasticizing agents were identified to further improve the above-mentioned properties. The loading of glycerol provided a conductivity of $(1.32 \pm 0.35) \times 10^{-3}$ S cm^{-1} for the chitosan-PS-LiCF$_3$SO$_3$ system [27].

In this study, glycerol (contains three OH groups) as an eligible plasticizer has been used in an effort to pick up the conductivity of the blended polymer system. It causes weakening of the attraction force between the polymer chains and cations and anions of the salts [4]. The objective of this study is to enhance the conductivity of the prepared SPEs by adding glycerol as more ions are dissociated to increase conductivity. The electrochemical tests indicate the films are convenient for applications.

2. Results and Discussion

2.1. FTIR Results

To study polymer-mix developments, several scientists have turned to FTIR. Intermolecular interactions may be studied using FTIR spectroscopy, which analyzes spectra based on the stretching or bending vibrations of specific bonds. Figure 1 showed the spectra of the electrolytes at the 400 to 4000 cm^{-1}. A wide band of 3353 cm^{-1} was observed in the FTIR spectra for MC: Dext, indicating the presence of OH groups [28,29]. The bands, due to -OH bending and -OH stretching, can be found at 1253–1503 cm^{-1} in a sharp peak and 3703–3149 cm^{-1} in a broad-peak form, respectively, by glycerol loading [30,31]. A peak at 1334 cm^{-1} came from -OH bending. The -CH asymmetrical and -CH symmetrical stretching are found at 3049 to 2849 cm^{-1} [32,33]. As the concentration of glycerol rises,

the intensity of the -CH bands increases, indicating a complicated interplay between the glycerol and MC-Dex-LiClO$_4$ [34]. As glycerol concentrations increase, the position of the electrolyte carboxamide and amine band shifts somewhat to 1749–1519 cm^{-1}. The impact of increasing the content of glycerol on the strength of the interaction between the components of the polymer blend is proved where additional ions are interacting with the oxygen atoms and nitrogen atoms [27]. The range of carboxamide and amine bands can be recognized straightforwardly as reported by Aziz et al. [35] and Shukur et al. [36]. Interestingly, a sharp peak lies between 901 and 1203 cm^{-1} that comes from the C-O stretching, which is in accordance with the findings of the study documented by Mejenom et al. [37]. This band peak widens as the glycerol concentration increases. The insertion of LiClO$_4$ salt into MC: Dex resulted in a significant shift in the strength of the bands, which is fascinating. The changes in the macromolecular arrangement have a direct effect on the intensity of these bands. The spectra of the complexes may show more and less organized structures, which might be the cause of these bands [38].
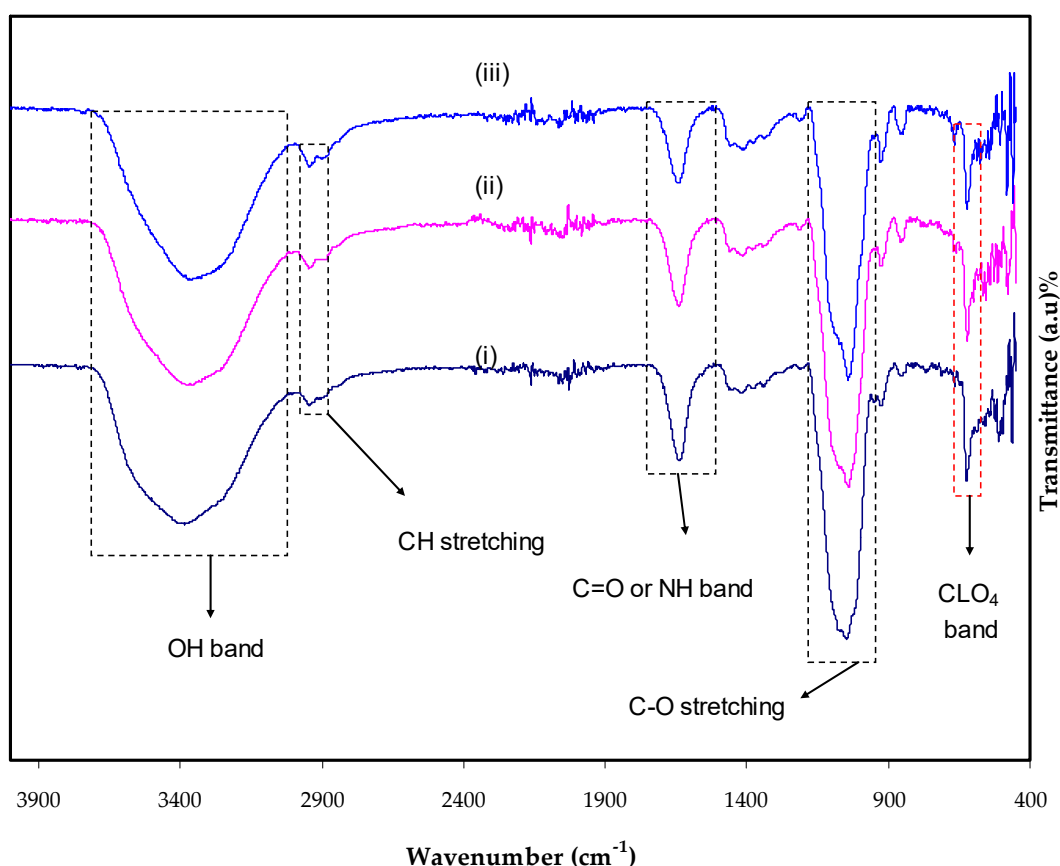

Figure 1. FTIR spectra for (i) MDLG1, (ii) MDLG2, and (iii) MDLG3 in the region 400–4000 cm^{-1}.

Many useful qualities, such as peak resolution, noise removal, and checking for interconnections between deconvolution parameters, are provided by the FTIR deconvolution, which is used in support of the conductivity findings [39]. When using this method, the deconvolution FTIR spectra may be used to determine the ion fraction that conducts electricity. Ramelli et al. noted that FTIR spectra might be deconvoluted, allowing one to isolate existing peaks and modify both intensity and wavenumber [40].

A peak for ClO$_4$ localizes from 650 to 600 cm^{-1} and is regularly utilized in the investigation of ion–ion interactions in the PE and LiClO$_4$ salt addition [41,42]. The ClO$_4$ bands are featured by two peaks extending from 610 to 630 cm^{-1}, which indicates that, at most, two dissimilar sorts of ClO$_4$ anions are present in this material.

Salomon et al. documented that the presence of Li^{+1} is attached to the ClO_4 band located at 610–630 cm^{-1}. CIP ClO_4^{-1} anions were observed at lower than 610 cm^{-1}, while free ClO_4 anions were observed at about 610–630 cm^{-1} [42]. Figure 2a–c show the deconvoluted FTIR spectra for the prepared electrolytes. The free ClO_4 peaks are larger than the peaks of contact-ion pairs, as shown in Figure 2. Glycerol plasticizer helps dissolve $LiClO_4$ salt in the MC: Dex matrix; therefore, this is what happens when the two mixtures are combined.
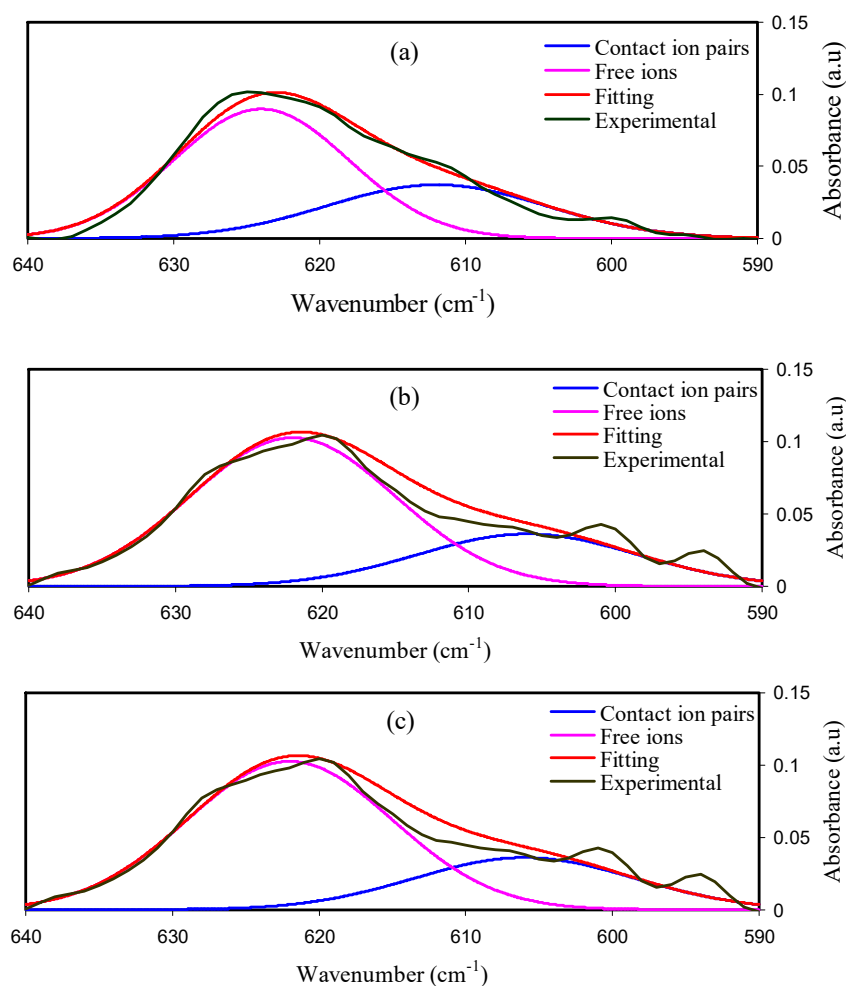

Figure 2. Deconvoluted FTIR spectra for (**a**) MDLG1, (**b**) MDLG2, and (**c**) MDLG3.

The free ions and contact ion pairs were measured using the area of the FTIR bands by the equations below [4]:

$$\text{Percentage of FI (\%)} = \frac{A_f}{A_f + A_c} \times 100\% \qquad (1)$$

$$\text{Percentage of CIP (\%)} = \frac{A_c}{A_f + A_c} \times 100\% \qquad (2)$$

where A_f is the area of the FIP and A_c is the area of the CIP. The percentages of FI and CIP are shown in Table 1.

Table 1. The percentages of ions.

Sample	FI%	CIP%
MDLG1	65.85%	34.14%
MDLG2	72.58%	27.42%
MDLG3	76.95%	23.05%

The rise in ionic conductivity might also be attributed to the rise in Li^+ ions that dissociate from $LiClO_4$ salts. There is a strong correlation between the conductivity and the proportion of free ions, according to Aniskari and colleagues [43]. The calculation of the number density (n), ionic mobility (μ), and diffusion coefficient (D) for each electrolyte can be calculated from Equations (3)–(5). In these equations, M stands for the molecular weight of glycerol and e is the electron charge, and N_A is the Avogadro's constant. A polymer electrolyte has a total volume of V_{Total}. The calculated values of n, μ, and D are shown in Table 2.

$$n = \frac{M \times N_A}{V_{Total}} \times (freeion\%) \tag{3}$$

$$\mu = \frac{\sigma}{ne} \tag{4}$$

$$D = \frac{\mu kT}{e} \tag{5}$$

Table 2. The n, D, and μ at ambient temperature from FTIR approach.

Glycerol %	n (cm^{-3})	μ (cm^2 V^{-1} s)	D (cm^2 s^{-1})
MDLG1	2.32×10^{22}	4.0×10^{-8}	1.04×10^{-9}
MDLG2	5.92×10^{22}	1.09×10^{-7}	2.83×10^{-9}
MDLG3	1.13×10^{23}	1.10×10^{-7}	2.86×10^{-9}

In Table 2 the D, μ and n values increase as the glycerol increases. The improvement of D and μ can be interpreted according to the increase in polymer chain flexibility upon the addition of the glycerol [1].

The relationship between the ionic conductivity of the electrolyte films and the ionic mobility is well-acknowledged and mathematically stated as follows:

$$\sigma = \sum \eta q \mu \tag{6}$$

where σ denotes the ionic conductivity, η represents the charge carrier density, and q stands for the single charge. From the equation above, it can be observed that the ionic conductivity improves with the increment of the ionic mobility as well as charge carrier density.

2.2. Impedance Study

Figure 3 shows the Cole-Cole plots used to estimate the impedance parameters of the electrolytes used in this study. An appropriate equivalent circuit model, with series connections for the resistor and the capacitor given by bulk resistance (R_b) and the constant phase element (CPE), is shown in the inset figure for each Cole-Cole plot. Ions flow via a resistor, whereas polymer chains remain immobile in a capacitor [44]. Because of the charge buildup and capacitive elements in the electrolytes, there is a spike in the plots created by the diffusion process inside the system [17,45]. This graph also shows how polarization and blocking electrodes in the Pes affect the inclination [46,47].
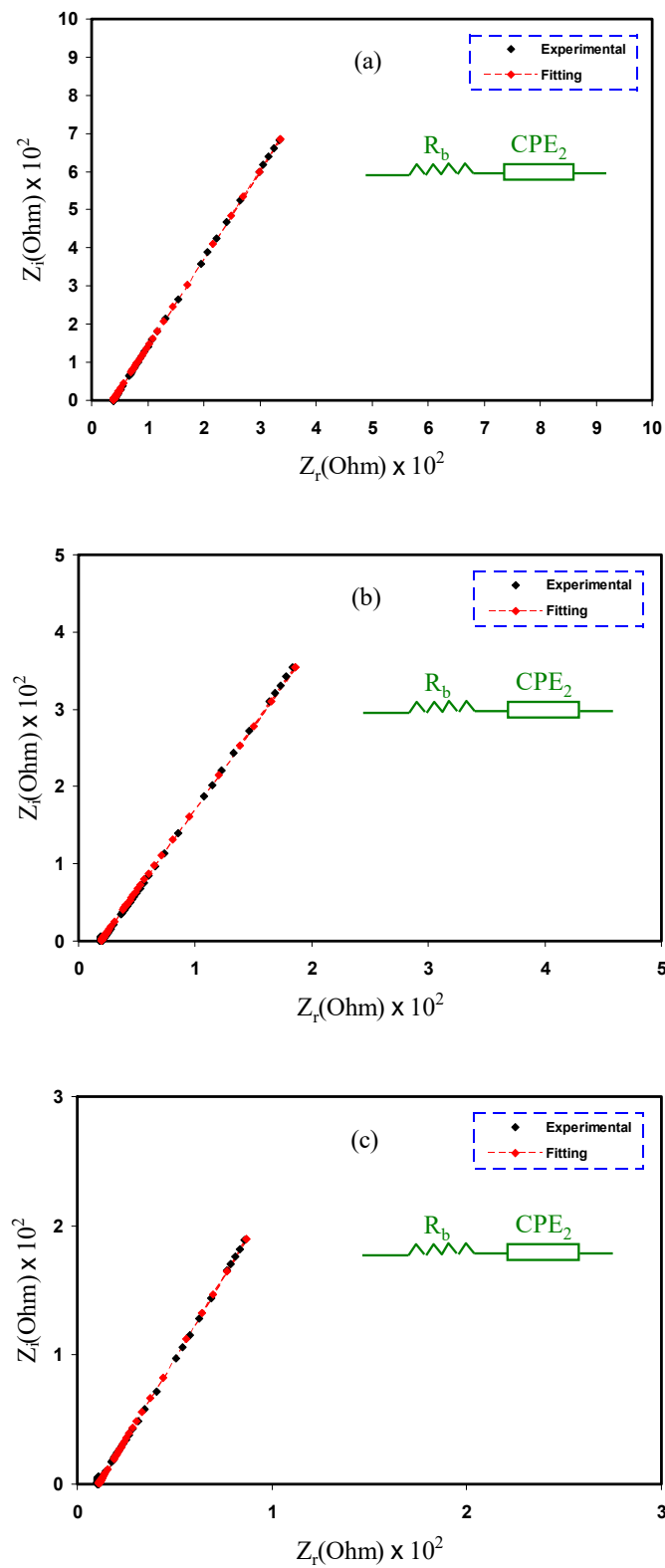
Figure 3. EIS spectra of (**a**) MDLG1, (**b**) MDLG2, and (**c**) MDLG3 electrolytes.

The impedance of *CPE* (Z_{CPE}) is written as follows [48,49]:

$$Z_{CPE} = \frac{1}{C\omega^p}\left[\cos\left(\frac{\pi p}{2}\right) - i\sin\left(\frac{\pi p}{2}\right)\right] \tag{7}$$

where ω denotes the angular frequency, p indicates the deviation of the plot from the axis, and C refers to the capacitance of *CPE* component. The spectra that involve only a spike and R_b are in series with *CPE*, and the real and the imaginary parts of impedance, Z_r and Z_i, are based on the following mathematical relationships.

$$Z_r = R + \frac{\cos\left(\frac{\pi p_2}{2}\right)}{C_2 \omega^{p2}} \tag{8}$$

$$Z_i = \frac{\sin\left(\frac{\pi p_2}{2}\right)}{C_2 \omega^{p2}} \tag{9}$$

The determined R_b and *CPE* for each electrolyte are listed in Table 3. The *CPE* values increase while the R_b values fall when glycerol concentrations increased. There are more ions in a solution, resulting in a higher capacitance value, which results in the greater mobility and dissociation of ions, thereby increasing conductivity [50,51]. The ionic conductivity (σ) measured using Equation (10) and also shown in Table 3 demonstrates this.

$$\sigma_{dc} = \left(\frac{1}{R_b}\right) \times \left(\frac{t}{A}\right) \tag{10}$$

Table 3. EEC fitting parameters for each sample.

Sample	K (F^{-1})	*CPE* (F)	R_b (Ohm)	Conductivity (S cm^{-1})
MDLG1	5.21×10^4	1.92×10^{-5}	3.80×10^1	3.93×10^{-4}
MDLG2	2.45×10^4	4.08×10^{-5}	1.89×10^1	8.16×10^{-4}
MDLG3	1.59×10^4	6.29×10^{-5}	1.10×10^1	1.45×10^{-3}

Here, t refers to the electrolyte's thickness; A denotes the SS electrodes area.

This study demonstrated that the MC:Dex:LiClO$_4$:glycerol combination is more flexible and mobile because of the glycerol [52]. The conductivity of 1.99×10^{-3} S cm^{-1}, achieved by MDLG3, is close to that achieved by Amran et al. [27] and Shukur et al. [30], and they also used glycerol as a plasticizer in their studies. It is also comparable with our previous studies of the biodegradable-blend-polymer electrolytes incorporated with ammonium salts [53,54]. The conductivity that was achieved in this study bodes well for future applications in energy devices [31].

As the samples have only a spike, D, μ, and n are measured by below equations [2]:

D is measured using Equations (11) and (12) [1]:

$$D = D_o \exp\left\{-0.0297[\ln D_o]^2 - 1.4348 \ln D_o - 14.504\right\} \tag{11}$$

where the following is the case.

$$D_o = \left(\frac{4k^2 l^2}{R_b{}^4 \omega_{\min}{}^3}\right) \tag{12}$$

Here, $\omega_{\min}$ and l correspond to the angular frequency that is based on the minimum Z_i and the electrolyte thickness, respectively. μ is measurable from the relationship shown in Equation (13):

$$\mu = \left(\frac{eD}{K_b T}\right) \tag{13}$$

where K_b and T are the Boltzmann constant possess normal meanings.

The conductivity can be measured using Equation (6).

Thus, the number n is measured using Equation (14):

$$n = \left(\frac{\sigma_{dc} K_b T \tau_2}{(e K_2 \varepsilon_o \varepsilon_r A)^2} \right) \tag{14}$$

In Table 4, D, μ, and n increased when glycerol increased. This is caused by increasing the polymer chain's flexibility when the glycerol is loaded [2]. The outcome shows how the concentration of glycerol affects the values of the ion number density, the ionic mobility, and the diffusion coefficient. This increase in D, μ, and n values can cause an increase in conductivity [4]. It is interesting to observe that when glycerol concentration increases, the number of ions (n) tends to increase continuously. Glycerol enhances the dissociation of salts to free ions; thus, n increases correspondingly. Meanwhile, ionic mobility (μ) and diffusion coefficient (D) are observed to follow the same trend of ionic conductivity, as shown in Table 3. The value of the free ion, which gradually increased by adding glycerol to the system, indicates that the ionic conductivity of the present system increased by the increasing the (n) value. These results from EIS and the FTIR deconvolution are in agreement.

Table 4. The values of ion transport parameters of each film from impedance approach.

Sample	D (cm^2 s^{-1})	μ (cm^2 V^{-1} s)	n (cm^{-3})
MDLG1	1.72×10^{-7}	6.71×10^{-6}	3.65×10^{20}
MDLG2	1.88×10^{-7}	7.33×10^{-6}	6.95×10^{20}
MDLG3	2.64×10^{-7}	1.03×10^{-5}	8.80×10^{20}

2.3. Dielectric Properties

According to current research, dielectric material qualities may be defined in multiple ways. There were many ways to increase the accuracy and sensitivity of material characterization [55–59]. Impedance studies at various frequencies have been shown to be a good approach for studying the molecular mobility of dielectric materials [60]. Dielectric studies may be used to examine the conductivity trend. Different amounts of glycerol at ambient temperature affect the dielectric constant (ε') and the dielectric loss (ε''), as observed in Figures 4 and 5, respectively. ε' and ε'' are measured using the equations below [61–63]:

$$\varepsilon' = \left[\frac{Z''}{\omega C_o (Z'^2 + Z''^2)} \right] \tag{15}$$

$$\varepsilon'' = \left[\frac{Z'}{\omega C_o (Z'^2 + Z''^2)} \right] \tag{16}$$

where C_o is the vacuum capacitance, which is equivalent to $\varepsilon_0 A / t$ in which ε_0 is the vacuum permittivity; the angular frequency is denoted by ω ($\omega = 2\pi f$); the frequency is denoted by f.

The conductivity of a polymer electrolyte is determined by its dielectric constant [64]. Real dielectric permittivity (ε') is used to determine the polarization or dipole alignment, which is measured by capacitance. Similarly to ε'', which indicates dielectric loss, conductance reflects the energy needed to align dipoles in a dielectric medium [65]. An important consideration in electrical conductivity testing is the identification of neutral ion pairs produced by the interaction of dissolved ion pairs [59]. In EIS measurements, it was shown that by adding more glycerol, the DC's conductivity significantly increased. ε' and ε'' at low frequencies are higher (Figures 4 and 5), which show variations for the films. Charge carriers or space charge polarization build up at the electrode/electrolyte contact point, causes this phenomenon [60]. Increasing the frequency reduces the dielectric property (bulk property). As a result, ε' and ε'' increase as a result of a decrease in the frequency of

the applied electric field [66]. As a result of the quick reversal of the electric field frequency, there is no new ion diffusion that takes place along its route, and polarization is reduced. Eventually, the peak shrinks to the point where it is no longer frequency dependent [48]. In a comparison to other samples, the system containing 42 wt.% of glycerol had a greater dielectric constant. Dielectric loss (ε'') and constant (ε') are strongly impacted by the conductivity in the system [51,67].
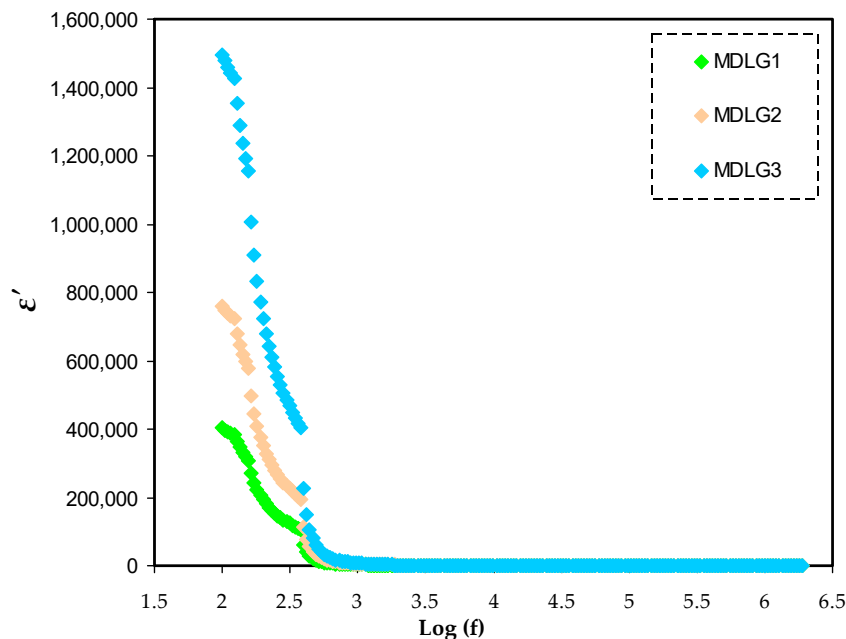
Figure 4. ε' spectra versus frequency for MC:Dex:LiClO$_4$:Glycerol electrolytes.

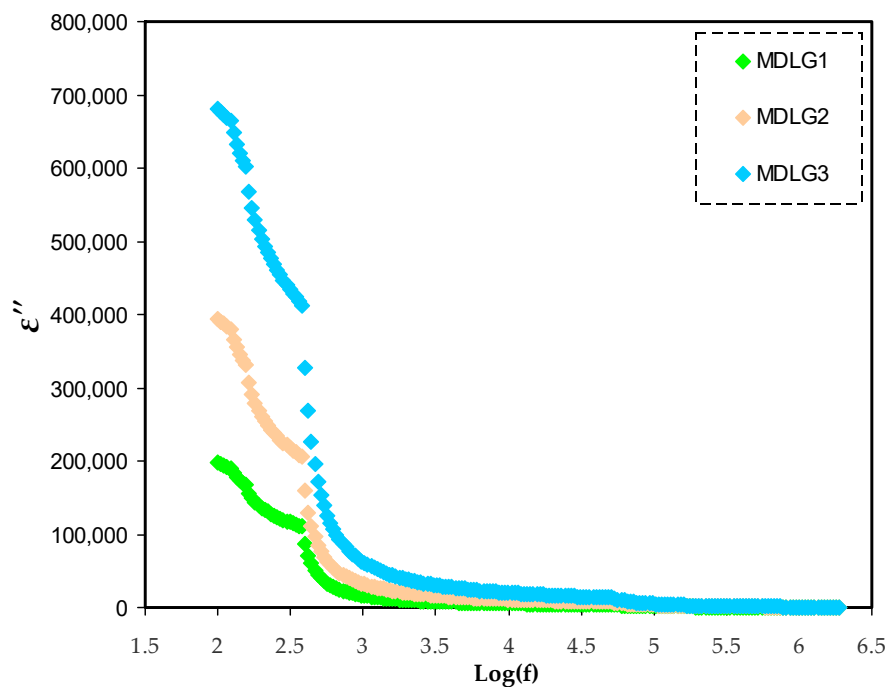**Figure 5.** ε'' spectra versus frequency for MC:Dex:LiClO$_4$:Glycerol electrolytes.

It has previously been observed that the dielectric constant (ε') and the density of the charge carriers (n_i) were formulated by the following relationship:

$$n_i = n_o \exp(-U/\varepsilon' K_b T) \tag{17}$$

where U is the dissociation energy.

DC's conductivity, as well as dielectric constant values, can be manipulated successfully [68]. The dielectric constants of polymer electrolytes may be used to determine the conductivity of certain materials and, hence, their electrical properties. A drop in dielectric constant is accompanied with a decrease in capacitance ($\varepsilon' = C/C_o$). The plots show that the ε'' value is higher than the ε', as shown in Figures 4 and 5. DC conduction processes and dielectric polarization processes both have an impact on dielectric loss [51].

2.4. TNM Study

In order to ensure the purely ionic nature of the PE system, the ion transport number (t_{ion}) has been measured for the optimized MC:Dex: LiClO$_4$:Glycerol composition using the DC polarization technique [69]. The curve obtained for the SS | Polymer electrolyte | SS cell (SS: stainless-steel) is shown in Figure 6. An initial current (I_i) of 128 A and the total of ionic and electronic currents were delivered by the cell. Since the SS electrode is ion-blocking in nature, the current declines quickly and is saturated at the residual electronic current (I_e) of 3 μA. The electrolyte system's ionic composition is thought to be responsible for the abrupt reduction in current levels. The t_{ion} and t_{el} values of the electrolyte film, obtained using the Equations (18) and (19), are found to be 0.976 and 0.024, respectively. These results show how ionic the electrolyte system is and how it will protect the electrodes of the energy storage device from each other since it is close to 1, which means it is close to the ideal value of unity. Ions are the key charge carriers in this system of methylcellulose-dextran-LiClO$_4$:Glycerol [70–72]. The result obtained in this study is observed to be high compared to our previous study for methylcellulose-based polymer electrolytes impregnated with potassium iodide [73].
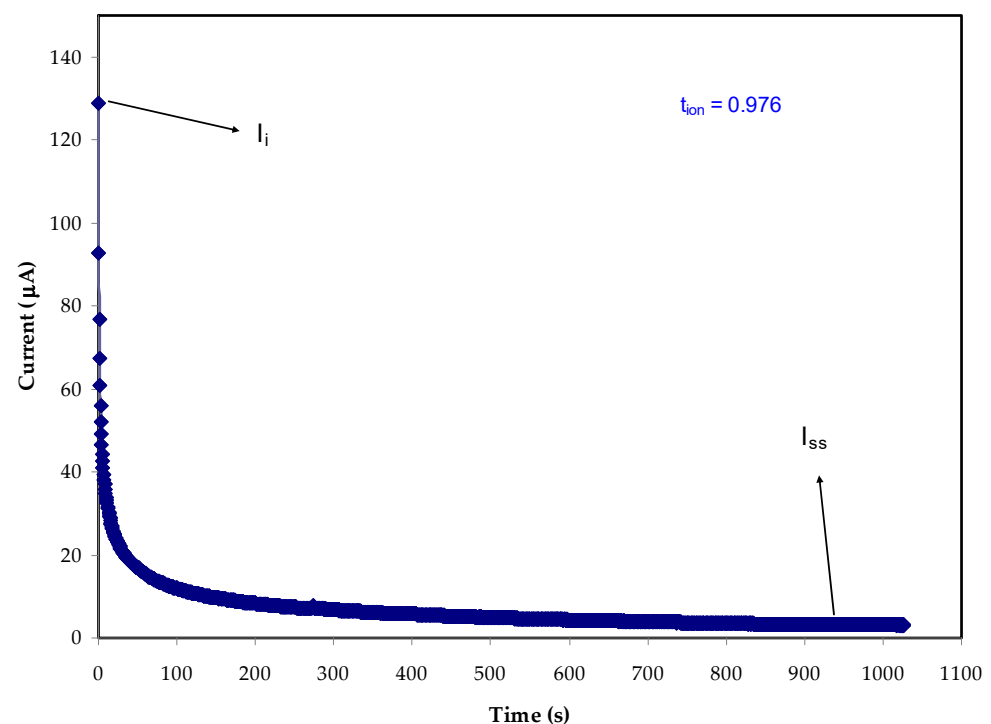

Figure 6. Chronoamperometric profile of for the MDLG3 electrolyte.

Equations (17) and (18) are used to measure t_{ion} and t_{el}.

$$t_{ion} = \frac{I_i - I_{ss}}{I_i} \tag{18}$$

$$t_{el} = 1 - t_{ion} \tag{19}$$

In Equations (18) and (19), the starting and the steady-state current are expressed as I_i and I_{ss}, respectively.

The electrochemical stability window (ESW) is an important parameter for an electrolyte, which determines the working voltage range of the energy storage device. The ESW of the optimized MC:Dextran:40 wt.% LiClO$_4$:48 wt.% Glycerol composition is obtained using linear sweep voltammetry (LSV). The LSV curve, shown in Figure 7, displays a plateau of negligible current without any anodic/cathodic current peak up to ~3 V. The present values increase sharply after the aforementioned potential. A considerable ESW of 3 V is shown, making the electrolyte film acceptable for supercapacitor use. In order for the film to be used in energy storage devices, the stability of the plasticized methylcellulose-dextran-LiClO$_4$ system has been shown to be up to 3 V. The interesting observation in this study is the eligibility of the MDLG3 electrolyte for energy storage device utilization. This is caused by the satisfactory voltage breakdown of the sample at almost 1.0 V [74,75]. The decomposition voltage attained in this study is relatively high compared to our previous studies [76,77]. This could be due to the presence of LiClO$_4$ as an ionic source, which has higher stability than ammonium salts. Moreover, a protic ionic liquid electrolyte was utilized for lithium-ion batteries as documented by Bockenfeld et al. [78]. They demonstrated that the highest potential stability was 2.65 V for their electrolyte that incorporated 0.5 M lithium nitrate (LiNO$_3$) in propylene carbonate-pyrrolidinium nitrate.
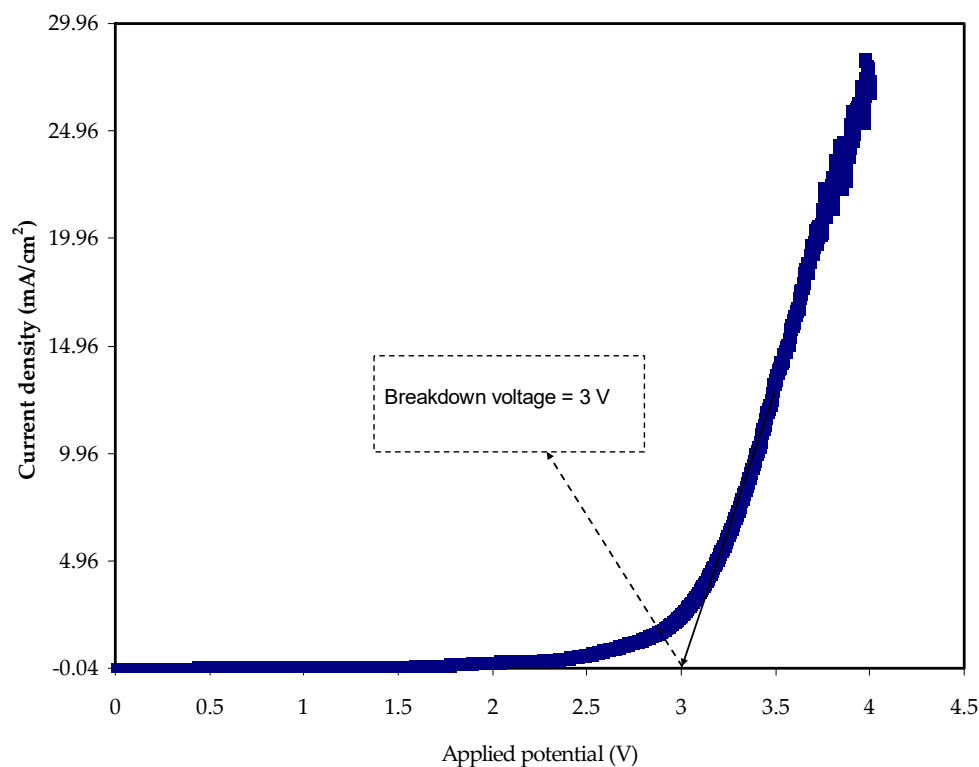

Figure 7. LSV for the MDLG3 film of SPE.

3. Materials and Methods

3.1. Materials

MC polymer ($M_{w\ avg}$ = 10,000–220,000), LiClO$_4$ (M_w = 106.39 g/mol) and glycerol (M_w = 92.09382 g/mol) were purchased from Sigma-Aldrich (Kuala Lumpur, Malaysia).

3.2. Electrolyte Preparation

The synthesis of MC-Dex-blend polymer was performed by stirring and dissolving 40 wt.% of Dex (0.4 g) and 60 wt.% of MC (0.6 g) individually, each in a 1% solution of

30 mL acetic acid, for almost 2 h at room temperature. Then, the two solutions were stirred and blended using a magnetic stirrer for around 4 h until reaching a homogenous-blend solution. Then, with respect to the above solution, 40 wt.% (0.666 g) of $LiClO_4$, MC-Dex-$LiClO_4$ formed. Ultimately, in the step of 14 wt.%, 14, 28, and 42 wt.% of glycerol were added to the MC-Dex-$LiClO_4$ solution followed by continuous stirring until the synthesis of plasticized SPEs was achieved. The labelling of the series of the samples was conducted as follows: MDLG1, MDLG2, and MDLG3 for the MC-Dex-$LiClO_4$ loading 14, 28, and 42 wt.% of glycerol, respectively as shown in Table 5. The casting of the series of sample solutions was carried out in the Petri dishes, followed by leaving them at room temperature to evaporate the solvent gradually. The free solvent sample films were kept in a desiccator.

Table 5. The identification and composition for the MC-Dex-$LiClO_4$–glycerol systems.

Sample Code	MC (g)	Dex (g)	$LiClO_4$ (g)	Glycerol (g)	Glycerol wt.%
MDLG1	0.6	0.4	0.666	0.271	14
MDLG2	0.6	0.4	0.666	0.647	28
MDLG3	0.6	0.4	0.666	1.206	42

3.3. Methods of Characterizations

3.3.1. FTIR and EIS Measurements

The FTIR spectra of the blended polymer systems were acquired using FTIR Spectrophotometer (Malvern Panalytical Ltd., Malvern, UK), ranging from 4000 to 400 cm^{-1} with a resolution of 2 cm^{-1}. The EIS samples spectra were acquired using the EIS (3532-50 LCR HiTESTER (HIOKI), Nagano, Japan) within 50 Hz and 5,000,000 Hz of frequency. The circle film had a geometric circle shape (diameter of 2 cm), which was sandwiched between stainless steel (SS) electrodes using a spring force during electrochemical measurements. The cell was hyphenated with a computer to measure real and imaginary (Z' and Z'') parts of the complex impedance spectra (Z^*).

3.3.2. TNM and LSV

The ion (t_{ion}) and electron (t_{el}) transference numbers were measured precisely. The cell (SS|MDLG3|SS) was connected to the UNI-T UT803 multimeter and A&V Instrument DP3003 digital DC power supply. By applying a voltage of 0.2 V to the cell, the polarization of the cell was obtained over a sufficient amount of time at room temperature. To obtain the potential stability of the MDLG3, LSV was used by applying 10 mV s^{-1} within 0.0 and 4.0 V. The cell was the three-electrode type, and the working, counter, and reference electrodes were used by utilizing the Digi-IVY DY2300 potentiostat. The current changes over the mentioned potential were obtained.

4. Conclusions

In this study, SPEs based on MC:Dex:$LiClO_4$ plasticized with glycerol were synthesized by the solution-cast method. The conductivity increased to 1.45×10^{-3} S cm^{-1} due to the doping of glycerol. The FTIR method showed that there was an interaction of $LiClO_4$ and glycerol with the MC and Dex by changing FTIR absorption peaks. The FTIR deconvolution of CLO_4^- anions showed that the free ion percentages increased when glycerol increased, while the percentages of contact ion pairs decreased. Further proof of *DC* conductivity trends was emphasized from the dielectric measurement. The addition of glycerol was effective in increasing the number density (*n*), diffusion coefficient (*D*), and mobility (*μ*). Additionally, the mass transport improvements of the electrolytes originate from the increase in chain flexibility. The values of measured t_{ion} and t_{el} indicate the ion's responsibility for conduction in the polymer-electrolyte system. The stability voltage range of the electrolyte system is satisfactory, meaning that the SPE is eligible for utilization at large scales in electrochemical energy storage devices.

References

1. Hadi, J.M.; Aziz, S.B.; Kadir, M.F.Z.; El-Badry, Y.A.; Ahamad, T.; Hussein, E.E.; Asnawi, A.S.F.M.; Abdullah, R.M.; Alshehri, S.M. Design of plasticized proton conducting Chitosan: Dextran based biopolymer blend electrolytes for EDLC application: Structural, impedance and electrochemical studies. *Arab. J. Chem.* **2021**, *14*, 103394. [CrossRef]
2. Hadi, J.M.; Aziz, S.B.; Brza, M.A.; Kadir, M.F.Z.; Abdulwahid, R.T.; Ali Al-Asbahi, B.; Ahmed Ali Ahmed, A. Structural and energy storage behavior of ion conducting biopolymer blend electrolytes based on methylcellulose: Dextran polymers. *Alex. Eng. J.* **2022**, *61*, 9273–9285. [CrossRef]
3. Alexandre, S.A.; Silva, G.G.; Santamaría, R.; Trigueiro, J.P.C.; Lavall, R.L. A highly adhesive PIL/IL gel polymer electrolyte for use in flexible solid state supercapacitors. *Electrochim. Acta* **2019**, *299*, 789–799. [CrossRef]
4. Brza, M.A.; Aziz, S.B.; Anuar, H.; Ali, F. Structural, Ion Transport Parameter and Electrochemical Properties of Plasticized Polymer Composite Electrolyte Based on PVA: A Novel Approach to Fabricate High Performance EDLC Devices. *Polym. Test.* **2020**, *91*, 106813. [CrossRef]
5. Nyuk, C.M.; Isa, M.I.N.M. Solid biopolymer electrolytes based on carboxymethyl cellulose for use in coin cell proton batteries. *J. Sustain. Sci. Manag.* **2017**, *2017*, 42–48.
6. Salleh, N.S.; Aziz, S.B.; Aspanut, Z.; Kadir, M.F.Z. Electrical impedance and conduction mechanism analysis of biopolymer electrolytes based on methyl cellulose doped with ammonium iodide. *Ionics* **2016**, *22*, 2157–2167. [CrossRef]
7. Hamsan, M.H.; Aziz, S.B.; Shukur, M.F.; Kadir, M.F.Z. Protonic cell performance employing electrolytes based on plasticized methylcellulose-potato starch-NH4NO3. *Ionics* **2019**, *25*, 559–572. [CrossRef]
8. Stepniak, I.; Galinski, M.; Nowacki, K.; Wysokowski, M.; Jakubowska, P.; Bazhenov, V.V.; Leisengang, T.; Ehrlich, H.; Jesionowski, T. A novel chitosan/sponge chitin origin material as a membrane for supercapacitors-preparation and characterization. *RSC Adv.* **2016**, *6*, 4007–4013. [CrossRef]
9. Sudhakar, Y.N.; Selvakumar, M.; Bhat, D.K. Preparation and characterization of phosphoric acid-doped hydroxyethyl cellulose electrolyte for use in supercapacitor. *Mater. Renew. Sustain. Energy* **2015**, *4*, 10. [CrossRef]
10. Hassan, M.F.; Azimi, N.S.N.; Kamarudin, K.H.; Sheng, C.K. Solid polymer electrolytes based on starch-Magnesium Sulphate: Study on morphology and electrical conductivity. *ASM Sci. J.* **2018**, *11*, 17–28.
11. Du, B.W.; Hu, S.Y.; Singh, R.; Tsai, T.T.; Lin, C.C.; Ko, F.H. Eco-friendly and biodegradable biopolymer chitosan/Y2O3 composite materials in flexible organic thin-film transistors. *Materials* **2017**, *10*, 1026. [CrossRef]
12. Moniha, V.; Alagar, M.; Selvasekarapandian, S.; Sundaresan, B.; Hemalatha, R.; Boopathi, G. Synthesis and characterization of bio-polymer electrolyte based on iota-carrageenan with ammonium thiocyanate and its applications. *J. Solid State Electrochem.* **2018**, *22*, 3209–3223. [CrossRef]
13. Hamsan, M.H.; Shukur, M.F.; Aziz, S.B.; Kadir, M.F.Z. Dextran from Leuconostoc mesenteroides-doped ammonium salt-based green polymer electrolyte. *Bull. Mater. Sci.* **2019**, *42*, 57. [CrossRef]
14. Nadirah, B.N.; Ong, C.C.; Saheed, M.S.M.; Yusof, Y.M.; Shukur, M.F. Structural and conductivity studies of polyacrylonitrile/methylcellulose blend based electrolytes embedded with lithium iodide. *Int. J. Hydrogen Energy* **2020**, *45*, 19590–19600. [CrossRef]
15. Salman, Y.A.K.; Abdullah, O.G.; Hanna, R.R.; Aziz, S.B. Conductivity and electrical properties of chitosan-methylcellulose blend biopolymer electrolyte incorporated with lithium tetrafluoroborate. *Int. J. Electrochem. Sci.* **2018**, *13*, 3185–3199. [CrossRef]

16. Simari, C.; Lufrano, E.; Coppola, L.; Nicotera, I. Composite gel polymer electrolytes based on organo-modified nanoclays: Investigation on lithium-ion transport and mechanical properties. *Membranes* **2018**, *8*, 69. [CrossRef]

17. Gohel, K.; Kanchan, D.K. Ionic conductivity and relaxation studies in PVDF-HFP:PMMA-based gel polymer blend electrolyte with LiClO$_4$ salt. *J. Adv. Dielectr.* **2018**, *8*, 1850005. [CrossRef]

18. Porcarelli, L.; Shaplov, A.S.; Salsamendi, M.; Nair, J.R.; Vygodskii, Y.S.; Mecerreyes, D.; Gerbaldi, C. Single-Ion Block Copoly(ionic liquid)s as Electrolytes for All-Solid State Lithium Batteries. *ACS Appl. Mater. Interfaces* **2016**, *8*, 10350–10359. [CrossRef]

19. Mantravadi, R.; Chinnam, P.R.; Dikin, D.A.; Wunder, S.L. High Conductivity, High Strength Solid Electrolytes Formed by in Situ Encapsulation of Ionic Liquids in Nanofibrillar Methyl Cellulose Networks. *ACS Appl. Mater. Interfaces* **2016**, *8*, 13426–13436. [CrossRef]

20. Weng, R.; Chen, L.; Lin, S.; Zhang, H.; Wu, H.; Liu, K.; Cao, S.; Huang, L. Preparation and characterization of antibacterial cellulose/chitosan nanofiltration membranes. *Polymers* **2017**, *9*, 116. [CrossRef] [PubMed]

21. Taghizadeh, M.T.; Seifi-Aghjekohal, P. Sonocatalytic degradation of 2-hydroxyethyl cellulose in the presence of some nanoparticles. *Ultrason. Sonochem.* **2015**, *26*, 265–272. [CrossRef]

22. Shuhaimi, N.E.A.; Teo, L.P.; Majid, S.R.; Arof, A.K. Transport studies of NH4NO3 doped methyl cellulose electrolyte. *Synth. Met.* **2010**, *160*, 1040–1044. [CrossRef]

23. Pinotti, A.; García, M.A.; Martino, M.N.; Zaritzky, N.E. Study on microstructure and physical properties of composite films based on chitosan and methylcellulose. *Food Hydrocoll.* **2007**, *21*, 66–72. [CrossRef]

24. Hamsan, M.H.; Shukur, M.F.; Kadir, M.F.Z. The effect of NH4NO3 towards the conductivity enhancement and electrical behavior in methyl cellulose-starch blend based ionic conductors. *Ionics* **2017**, *23*, 1137–1154. [CrossRef]

25. Kadir, M.; Hamsan, M. Green electrolytes based on dextran-chitosan blend and the effect of NH4SCN as proton provider on the electrical response studies. *Ionics* **2018**, *24*, 2379–2398. [CrossRef]

26. Yang, P.; Liu, L.; Li, L.; Hou, J.; Xu, Y.; Ren, X.; An, M.; Li, N. Gel polymer electrolyte based on polyvinylidenefluoride-co-hexafluoropropylene and ionic liquid for lithium ion battery. *Electrochim. Acta* **2014**, *115*, 454–460. [CrossRef]

27. Amran, N.N.A.; Manan, N.S.A.; Kadir, M.F.Z. The effect of LiCF3SO3 on the complexation with potato starch-chitosan blend polymer electrolytes. *Ionics* **2016**, *22*, 1647–1658. [CrossRef]

28. Vettori, M.H.P.B.; Franchetti, S.M.M.; Contiero, J. Structural characterization of a new dextran with a low degree of branching produced by Leuconostoc mesenteroides FT045B dextransucrase. *Carbohydr. Polym.* **2012**, *88*, 1440–1444. [CrossRef]

29. Dumitra, M.; Meltze, V. Characterization of electron beam irradiated collagen-polyvinylpyrrolidone (PVP) and collagen-dextran (DEX) blends. *Dig. J. Nanomater. Biostruct.* **2011**, *6*, 1793–1803.

30. Shukur, M.F.; Kadir, M.F.Z. Electrical and transport properties of NH4Br-doped cornstarch-based solid biopolymer electrolyte. *Ionics* **2015**, *21*, 111–124. [CrossRef]

31. Aziz, S.B.; Brza, M.A.; Brevik, I.; Hafiz, M.H.; Asnawi, A.S.; Yusof, Y.M.; Abdulwahid, R.T.; Kadir, M.F.Z. Blending and characteristics of electrochemical double-layer capacitor device assembled from plasticized proton ion conducting chitosan:Dextran:NH4PF6 polymer electrolytes. *Polymers* **2020**, *12*, 2103. [CrossRef] [PubMed]

32. Ndruru, S.T.C.L.; Wahyuningrum, D.; Bundjali, B.; Arcana, I.M. Preparation and characterization of biopolymer electrolyte membranes based on liclo4-complexed methyl cellulose as lithium-ion battery separator. *J. Eng. Technol. Sci.* **2020**, *52*, 28–50. [CrossRef]

33. Hafiza, M.N.; Isa, M.I.N. Correlation between structural, ion transport and ionic conductivity of plasticized 2-hydroxyethyl cellulose based solid biopolymer electrolyte. *J. Memb. Sci.* **2020**, *597*, 117176. [CrossRef]

34. Aziz, S.B.; Dannoun, E.M.A.; Murad, A.R.; Mahmoud, K.H.; Brza, M.A.; Nofal, M.M.; Elsayed, K.A.; Abdullah, S.N.; Hadi, J.M.; Kadir, M.F.Z. Influence of scan rate on CV Pattern: Electrical and electrochemical properties of plasticized Methylcellulose: Dextran (MC:Dex) proton conducting polymer electrolytes. *Alex. Eng. J.* **2022**, *61*, 5919–5937. [CrossRef]

35. Aziz, S.B.; Hamsan, M.H.; MNofal, M.; Karim, W.O.; Brevik, I.; Brza, M.; Abdulwahid, R.T.; Al-Zangana, S.; Kadir, M.F.Z. Structural, Impedance and Electrochemical Characteristics of Electrical Double Layer Capacitor Devices Based on Chitosan: Dextran Biopolymer Blend Electrolytes. *Polymers* **2020**, *12*, 1411. [CrossRef]

36. Shukur, M.F.; Azmi, M.S.; Zawawi, S.M.M.; Majid, N.A.; Illias, H.A.; Kadir, M.F.Z. Conductivity studies of biopolymer electrolytes based on chitosan incorporated with NH4Br. *Phys. Scr.* **2013**, *2013*, 014049. [CrossRef]

37. Mejenom, A.A.; Hafiza, M.N.; Isa, M.I.N. X-Ray diffraction and infrared spectroscopic analysis of solid biopolymer electrolytes based on dual blend carboxymethyl cellulose-chitosan doped with ammonium bromide. *ASM Sci. J.* **2018**, *11*, 37–46.

38. Aziz, S.B.; Marif, R.B.; Brza, M.A.; Hassan, A.N.; Ahmad, H.A.; Faidhalla, Y.A.; Kadir MF, Z. Structural, thermal, morphological and optical properties of PEO filled with biosynthesized Ag nanoparticles: New insights to band gap study. *Results Phys.* **2019**, *13*, 102220. [CrossRef]

39. Pistorius, A.M.A.; DeGrip, W.J. Deconvolution as a tool to remove fringes from an FT-IR spectrum. *Vib. Spectrosc.* **2004**, *36*, 89–95. [CrossRef]

40. Ramlli, M.A.; Bashirah, N.A.A.; Isa, M.I.N. Ionic Conductivity and Structural Analysis of 2-hyroxyethyl Cellulose Doped with Glycolic Acid Solid Biopolymer Electrolytes for Solid Proton Battery. In *IOP Conference Series: Materials Science and Engineering*; IOP Publishing: Bristol, UK, 2018; Volume 440, p. 012038. [CrossRef]

41. Xi, J.; Bai, Y.; Qiu, X.; Zhu, W.; Chen, L.; Tang, X. Conductivities and transport properties of microporous molecular sieves doped composite polymer electrolyte used for lithium polymer battery. *New J. Chem.* **2005**, *29*, 1454–1460. [CrossRef]

42. Abarna, S.; Hirankumar, G. Electrical, dielectric and electrochemical studies on new Li ion conducting solid polymer electrolytes based on polyethylene glycol p-tert-octylphenyl ether. *Polym. Sci. Ser. A* **2017**, *59*, 660–668. [CrossRef]

43. Aniskari, N.A.B.; Isa, M.I.N.M. The effect of ionic charge carriers in 2-hydroxyethyl cellulose solid biopolymer electrolytes doped glycolic acid via FTIR-deconvolution technique. *J. Sustain. Sci. Manag.* **2017**, *12*, 71–79.

44. Kumar, M.; Tiwari, T.; Chauhan, J.K.; Srivastava, N. Erratum: UnderstanDing the ion dynamics and relaxation behavior from impedance spectroscopy of NaI doped Zwitterionic polymer system (Materials Research Express (2013) 1 (045003)). *Mater. Res. Express* **2014**, *1*, 045003. [CrossRef]

45. Samsudin, A.S.; Khairul, W.M.; Isa, M.I.N. Characterization on the potential of carboxy methylcellulose for application as proton conducting biopolymer electrolytes. *J. Non. Cryst. Solids* **2012**, *358*, 1104–1112. [CrossRef]

46. Fonseca, C.P.; Cavalcante, F.; Amaral, F.A.; Souza, C.A.Z.; Neves, S. Thermal and conduction properties of a PCL-biodegradable gel polymer electrolyte with LiClO$_4$, LiF$_3$CSO$_3$, and LiBF$_4$ salts. *Int. J. Electrochem. Sci.* **2007**, *2*, 52–63.

47. Misenan, M.; Khiar, A. Conductivity, Dielectric And Modulus Studies of Methylcellulose-NH 4 TF Polymer. *Eurasian J. Biol. Chem. Sci. J.* **2018**, *1*, 59–62.

48. Teo, L.P.; Buraidah, M.H.; Nor, A.F.M.; Majid, S.R. Conductivity and dielectric studies of Li$_2$SnO$_3$. *Ionics* **2012**, *18*, 655–665. [CrossRef]

49. Aziz, S.B.; Marif, R.B.; Brza, M.A.; Hamsan, M.H.; Kadir, M.F.Z. Employing of Trukhan model to estimate ion transport parameters in PVA based solid polymer electrolyte. *Polymers* **2019**, *11*, 1694. [CrossRef]

50. Lee, D.K.; Allcock, H.R. The effects of cations and anions on the ionic conductivity of poly[bis(2-(2-methoxyethoxy)ethoxy) phosphazene] doped with lithium and magnesium salts of trifluoromethanesulfonate and bis(trifluoromethanesulfonyl)imidate. *Solid State Ionics* **2010**, *181*, 1721–1726. [CrossRef]

51. Awasthi, P.; Das, S. Reduced electrode polarization at electrode and analyte interface in impedance spectroscopy using carbon paste and paper. *Rev. Sci. Instrum.* **2019**, *90*, 124103. [CrossRef]

52. Marf, A.S.; Aziz, S.B.; Abdullah, R.M. Plasticized H+ ion-conducting PVA:CS-based polymer blend electrolytes for energy storage EDLC application. *J. Mater. Sci. Mater. Electron.* **2020**, *31*, 18554–18568. [CrossRef]

53. Aziz, S.B.; Ali, F.; Anuar, H.; Ahamad, T.; Kareem, W.O.; Brza, M.A.; Kadir, M.F.Z.; Abu Ali, O.A.; Saleh, D.I.; Asnawi, A.S.F.M.; et al. Structural and electrochemical studies of proton conducting biopolymer blend electrolytes based on MC:Dextran for EDLC device application with high energy density. *Alex. Eng. J.* **2022**, *61*, 3985–3997. [CrossRef]

54. Aziz, S.B.; Hadi, J.M.; Elham, E.M.; Abdulwahid, R.T.; Saeed, S.R.; Marf, A.S.; Karim, W.O.; Kadir, M.F.Z. The study of plasticized amorphous biopolymer blend electrolytes based on polyvinyl alcohol (PVA): Chitosan with high ion conductivity for energy storage electrical double-layer capacitors (EDLC) device application. *Polymers* **2020**, *12*, 1938. [CrossRef]

55. Uğuz, H.; Goyal, A.; Meenpal, T.; Selesnick, I.W.; Baraniuk, R.G.; Kingsbury, N.G.; Haiter Lenin, A.; Mary Vasanthi, S.; Jayasree, T.; Adam, M.; et al. ce pte d M us pt. *J. Phys. Energy* **2020**, *2*, 1–31.

56. Al-Omari, A.N.; Lear, K.L. Dielectric characteristics of spin-coated dielectric films using on-wafer parallel-plate capacitors at microwave frequencies. *IEEE Trans. Dielectr. Electr. Insul.* **2005**, *12*, 1151–1161. [CrossRef]

57. Park, S.J.; Yoon, S.A.N.; Ahn, Y.H. Dielectric constant measurements of thin films and liquids using terahertz metamaterials. *RSC Adv.* **2016**, *6*, 69381–69386. [CrossRef]

58. Anderson, L.; Jacob, M. Microwave characterization of a novel, environmentally friendly, plasma polymerized organic thin film. *Phys. Procedia* **2011**, *14*, 87–90. [CrossRef]

59. Aziz, S.B.; Mamand, S.M.; Saed, S.R.; Abdullah, R.M.; Hussein, S.A. New Method for the Development of Plasmonic Metal-Semiconductor Interface Layer: Polymer Composites with Reduced Energy Band Gap. *J. Nanomater.* **2017**, *2017*, 060803. [CrossRef]

60. Aziz, S.B.; Kadir, M.F.Z.; Hamsan, M.H.; Woo, H.J.; Brza, M.A. Development of Polymer Blends Based on PVA:POZ with Low Dielectric Constant for Microelectronic Applications. *Sci. Rep.* **2019**, *9*, 13163. [CrossRef]

61. Hadi, J.M.; Aziz, S.B.; Saeed, S.R.; Brza, M.A.; Abdulwahid, R.T.; Hamsan, M.H.; Abdullah, R.M.; Kadir, M.F.Z.; Muzakir, S.K. Investigation of ion transport parameters and electrochemical performance of plasticized biocompatible chitosan-based proton conducting polymer composite electrolytes. *Membranes* **2020**, *10*, 363. [CrossRef]

62. Hadi, J.M.; Aziz, S.B.; Mustafa, M.S.; Hamsan, M.H.; Abdulwahid, R.T.; Kadir, M.F.Z.; Ghareeb, H.O. Role of nano-capacitor on dielectric constant enhancement in PEO:NH$_4$SCN:xCeO$_2$ polymer nano-composites: Electrical and electrochemical properties. *J. Mater. Res. Technol.* **2020**, *9*, 9283–9294. [CrossRef]

63. Hadi, J.M.; Aziz, S.B.; Mustafa, M.S.; Brza, M.A.; Hamsan, M.H.; Kadir, M.F.Z.; Ghareeb, H.O.; Hussein, S.A. Electrochemical Impedance study of Proton Conducting Polymer Electrolytes based on PVC Doped with Thiocyanate and Plasticized with Glycerol. *Int. J. Electrochem. Sci.* **2020**, *15*, 4671–4683. [CrossRef]

64. Tamilselvi, P.; Hema, M. Structural, thermal, vibrational, and electrochemical behavior of lithium ion conducting solid polymer electrolyte based on poly(vinyl alcohol)/poly(vinylidene fluoride) blend. *Polym. Sci. Ser. A* **2016**, *58*, 776–784. [CrossRef]

65. Aziz, S.B.; Brza, M.A.; Mohamed, P.A.; Kadir MF, Z.; Hamsan, M.H.; Abdulwahid, R.T.; Woo, H.J. Increase of metallic silver nanoparticles in Chitosan:AgNt based polymer electrolytes incorporated with alumina filler. *Results Phys.* **2019**, *13*, 102326. [CrossRef]

66. Aziz, S.B.; Abdullah, R.M. Crystalline and amorphous phase identification from the tanδ relaxation peaks and impedance plots in polymer blend electrolytes based on [CS:AgNt]x:PEO(x−1) (10 ≤ x ≤ 50). *Electrochim. Acta* **2018**, *285*, 30–46. [CrossRef]

67. Khiar, A.S.A.; Anuar, M.R.S.; Parid, M.A.M. Effect of 1-ethyl-3-methylimidazolium nitrate on the electrical properties of starch/chitosan blend polymer electrolyte. *Mater. Sci. Forum* **2016**, *846*, 510–516. [CrossRef]

68. Aziz, S.B.; Rasheed, M.A.; Abidin, Z.H.Z. Optical and Electrical Characteristics of Silver Ion Conducting Nanocomposite Solid Polymer Electrolytes Based on Chitosan. *J. Electron. Mater.* **2017**, *46*, 6119–6130. [CrossRef]

69. Aziz, S.B.; Asnawi, A.S.F.M.; Abdulwahid, R.T.; Ghareeb, H.O.; Alshehri, S.M.; Ahamad, T.; Hadi, J.M.; Kadir, M.F.Z. Design of potassium ion conducting PVA based polymer electrolyte with improved ion transport properties for EDLC device application. *J. Mater. Res. Technol.* **2021**, *13*, 933–946. [CrossRef]

70. Nofal, M.M.; Aziz, S.B.; Brza, M.A.; Abdullah, S.N.; Dannoun, E.M.A.; Hadi, J.M.; Murad, A.R.; Al-Saeedi, S.I.; Kadir, M.F.Z. Studies of Circuit Design, Structural, Relaxation and Potential Stability of Polymer Blend Electrolyte Membranes Based on PVA:MC Impregnated with NH4I Salt. *Membranes* **2022**, *12*, 284. [CrossRef]

71. Nofal, M.M.; Hadi, J.M.; Aziz, S.B.; Brza, M.A.; Asnawi, A.S.F.M.; Dannoun, E.M.A.; Abdullah, A.M.; Kadir, M.F.Z. A Study of Methylcellulose Based Polymer Electrolyte Impregnated with Potassium Ion Conducting Carrier: Impedance, EEC Modeling, FTIR, Dielectric, and Device Characteristics. *Materials* **2021**, *14*, 4859. [CrossRef]

72. Hadi, J.M.; Aziz, S.B.; Nofal, M.M.; Hussein, S.A.; Hamsan, M.H.; Brza, M.A.; Abdulwahid, R.T.; Kadir, M.F.Z.; Woo, H.J. Electrical, Dielectric Property and Electrochemical Performances of Plasticized Silver Ion-Conducting Chitosan-Based Polymer Nanocomposites. *Membranes* **2020**, *10*, 151. [CrossRef] [PubMed]

73. Aziz, S.B.; Dannoun, E.M.A.; Hamsan, M.H.; Ghareeb, H.O.; Nofal, M.M.; Karim, W.O.; Asnawi, A.S.F.M.; Hadi, J.M.; Kadir, M.F.Z.A. A Polymer Blend Electrolyte Based on CS with Enhanced Ion Transport and Electrochemical Properties for Electrical Double Layer Capacitor Applications. *Polymers* **2021**, *13*, 930. [CrossRef] [PubMed]

74. Shuhaimi, N.E.A.; Alias, N.A.; Majid, S.R.; Arof, A.K. Electrical Double Layer Capacitor With Proton Conducting κ-Carrageenan–Chitosan Electrolytes. *Funct. Mater. Lett.* **2009**, *1*, 195–201. [CrossRef]

75. Mazuki, N.; Majeed, A.P.P.A.; Samsudin, A.S. Study on electrochemical properties of CMC-PVA doped NH4Br based solid polymer electrolytes system as application for EDLC. *J. Polym. Res.* **2020**, *27*, 135. [CrossRef]

76. Aziz, S.B.; Nofal, M.M.; Kadir, M.F.Z.; Dannoun, E.M.A.; Brza, M.A.; Hadi, J.M.; Abdullah, R.M. Bio-Based Plasticized PVA Based Polymer Blend Electrolytes for Energy Storage EDLC Devices: Ion Transport Parameters and Electrochemical Properties. *Materials* **2021**, *14*, 1994. [CrossRef]

77. Aziz, S.B.; Nofal, M.M.; Abdulwahid, R.T.; Kadir, M.F.Z.; Hadi, J.M.; Hessien, M.M.; Kareem, W.O.; Dannoun, E.M.A.; Saeed, S.R. Impedance, FTIR and transport properties of plasticized proton conducting biopolymer electrolyte based on chitosan for electrochemical device application. *Results Phys.* **2021**, *29*, 104770. [CrossRef]

78. Böckenfeld, N.; Willeke, M.; Pires, J.; Anouti, M.; Balducci, A. On the Use of Lithium Iron Phosphate in Combination with Protic Ionic Liquid-Based Electrolytes. *J. Electrochem. Soc.* **2013**, *160*, A559–A563. [CrossRef]